

Dentin Matrix Protein 1 Regulates Mineralization of MC3T3-E1 Cells via the TNAP-ANK-ENPP1 Axis

Jianmin Liu^{1,2,#}, Juhua Zhao^{1,#}, Zhi Li¹, Hongmei Wang³,
Binbin Wang¹, Wei Liu¹ and Lei Zhou¹

¹Allergy and Clinical Immunology Research Centre, the First Affiliated Hospital of Jinzhou Medical University, Liaoning, P. R. China

²Jinzhou Palmtop Cloud Biotechnology Co., Ltd., Liaoning, P. R. China

³Department of Clinical Laboratory, The First Affiliated Hospital of Jinzhou Medical University, Liaoning, P. R. China

Background: Dentin matrix protein 1 (DMP1) is central to matrix mineralization. Clarification of the function of DMP1 is crucial to understanding normal bone formation and pathological calcification. The tissue-nonspecific alkaline phosphatase (TNAP)-progressive ankylosing enzyme (ANK)-extracellular nucleotide pyrophosphatase/phosphodiesterase-1 (ENPP1) axis induces deposition of hydroxyapatite (HA) and pyrophosphate dehydrate (CPPD) by regulating pyrophosphate (PPi). Here, we investigated the mechanism by which DMP1 and the TNAP-ANK-ENPP1 axis participate in mineralization.

Methods: Expression of DMP1, TNAP, NPP1, and ANK genes in MC3T3-E1 cells was detected by RT-qPCR before and after treatment with DMP1 siRNA. An enzyme-linked immunosorbent assay was used to determine expression of DMP1 protein, TNAP activity was detected by SIGMAFAST p-nitrophenyl phosphate tablets, and mineralization of osteoblasts was determined by alizarin red staining. PPi levels were determined radiometrically and equalized for cell DNA. Levels of calcium, inorganic phosphate, zinc, and magnesium were assessed by standard laboratory techniques.

Results: After DMP1 gene silencing, expressions of TNAP, ENPP1, and ANK were correspondingly reduced. DMP1 altered extravesicular and intravesicular ion levels through the TNAP-ENPP1-ANK axis in MC3T3-E1 cells.

Conclusions: DMP1 regulated mineralization of MC3T3-E1 cells via the TNAP-ANK-ENPP1 axis and affected TNAP activity by two processes—rapid regulation of the Zn²⁺ transporter (ZnT) and transcriptional regulation of hysteresis. However, DMP1 may affect expression of ENPP1 and ANK only via hysteresis transcriptional regulation. DMP1, as a calcium trap or catalytic enzyme, appears to have a role in collagen mineralization. (*J Nippon Med Sch* 2023; 90: 262–271)

Key words: DMP1, TNAP-ANK-ENPP1 axis, mineralization, Pi/PPi-TNAP-positive feedback

Introduction

Mineralization is a tightly regulated process determined by extracellular matrix (ECM) proteins, ion channels, proteinases, and other promoter and inhibitor molecules. A better understanding of physiological mineralization and the effect of anti-calcification drugs on the mechanisms of mineralization could provide useful information for targeting and treating pathological calcification, defined as

deposition of minerals in soft tissues that do not normally mineralize, or premature or excessive calcification of normal mineralized tissues. Many diseases are associated with pathological mineralization/ossification, including ankylosing spondylitis (AS), osteoarthritis (OA), chondrocalcinosis (CC), and pseudogout. AS and OA are mainly characterized by mineralization/ossification associated with hydroxyapatite (HA) deposits¹, while CC and

[#] These authors contributed equally to this work and should be considered co-first authors.

Correspondence to Lei Zhou, Allergy and Clinical Immunology Research Centre, the First Affiliated Hospital of Jinzhou Medical University, No. 2, Section 5 Renmin Street, Guta District, Jinzhou, Liaoning 121001, People's Republic of China

E-mail: Angela_xiaolei@163.com

https://doi.org/10.1272/jnms.JNMS.2023_90-306

Journal Website (<https://www.nms.ac.jp/sh/jnms/>)

pseudogout are primarily characterized by pyrophosphate dehydrate (CPPD) deposits^{2,3}.

Dentin matrix protein 1 (DMP1), a non-collagenous ECM protein, is central to matrix mineralization in the formation of dentin and bone. DMP1 is expressed by odontoblasts and osteoblasts and appears to be crucial for matrix mineralization by regulating crystal size and morphology⁴. Using Fourier transform infrared imaging analysis, Ling et al.⁵ and Liu et al.⁶ found that DMP1 depletion decreased bone mineralization *in vivo*. Moreover, studies by Narayanan et al.⁷, Bhatia et al.⁸ and Merkel et al.⁹ demonstrated that overexpression or endocytic trafficking of DMP1 could induce differentiation of pluripotent and mesenchymal-derived cells and accelerate mineralization to form functional odontoblast-like cells. Taken together, these results suggest that DMP1 has a regulatory function during the formation of the mineralized matrix. Additionally, our previous results indicated that the DMP1 gene is involved in the genetic predisposition to AS in a Chinese Han population from Shandong Province and may contribute to ectopic mineralization or ossification in AS¹⁰.

Tissue-nonspecific alkaline phosphatase (TNAP) is an important promoter of mineralization and a well-characterized marker of the osteoblast lineage¹¹. Liu et al.¹² highlighted the importance of the HLA-B27-mediated activation of TNAP in AS syndesmophyte pathogenesis. The progressive ankylosing enzyme (ANK) is a transmembrane protein that plays a crucial role in the incorporation of pyrophosphate (PPi) in the mineralized bone matrix. ANK regulates transport of intracellular PPi to the extracellular space^{13,14} and offsets the activity of TNAP by increasing extracellular PPi levels by providing a substrate for extracellular nucleotide pyrophosphatase/phosphodiesterase-1 (ENPP1)¹⁵. Loss of ANK function results in decreased extracellular PPi. ENPP1 is present on the cell surface and in cytoplasm and generates PPi in both regions^{16,17}. The TNAP-ANK-ENPP1 axis induces HA and CPPD deposition by regulating PPi. The actions of TNAP, ENPP1, and ANK maintain the proper PPi/Pi ratio, which is directly related to mineralization: a high PPi/Pi ratio inhibits mineralization, whereas a low PPi/Pi ratio promotes mineralization. However, the mechanism by which DMP1 and the TNAP-ANK-ENPP1 axis participate in mineralization are unknown. Here, we investigated the precise mechanism by which DMP1 and the TNAP-ANK-ENPP1 axis, including TNAP, ANK, and ENPP1, participate in mineralization in cultured MC3T3-E1 cells.

It is important to gain a firm understanding of the mechanisms involved in the regulation of physiological mineralization before attempting to generate novel therapeutics for treating pathological calcification. MC3T3-E1, a well-established preosteoblast cell line, is widely used as an *in vitro* model of osteogenesis that reproduces *in vivo* conditions. Using the MC3T3-E1 murine preosteoblast cell line, we examined whether there is a direct effect of DMP1 on the regulation of PPi and whether the TNAP-ANK-ENPP1 axis is involved in this response.

Materials and Methods

Cell Culture and Transfection

MC3T3-E1 mouse preosteoblastic cells obtained from American Type Culture Collection (Manassas, VA, USA) were cultured in Dulbecco's modified Eagle's medium supplemented with 1% penicillin and streptomycin (Gibco, Gaithersburg, MD, USA) and 10% heat-inactivated fetal bovine serum (HyClone, Logan, UT, USA). Stable transfections with small interfering RNA (siRNA) and blank siRNA were performed using Lipofectamine RNAiMAX (Life Technologies Invitrogen, Carlsbad, CA, USA) according to the manufacturer's protocol. Transfections were performed on cells at 80-85% confluence in six-well plates. The efficacy of transfection was evaluated via observation of red fluorescent cells versus total cells with a fluorescence microscope. The experiments were repeated at least three times. The sequence of the siRNA-DMP1 was 5'-GGACGGUUCUGAGUUCGAUGAUGA-3'.

Morphological Observations

The cells were evaluated under a phase-contrast microscope. Microphotographs were taken with a Nikon camera and a 310 objective lens (Nikon, Tokyo, Japan).

Real-Time Quantitative Reverse Transcription Polymerase Chain Reaction

Total RNA was isolated from osteoblasts by using 0.5 mL TRIzol (Life Technologies) in a 35-mm dish. For each sample, total RNA content was assessed by absorbance at 260 nm, and the purity of the RNA was assessed by the A260/A280 ratio, measured using a NanoDrop spectrophotometer (Fischer Scientific, Loughborough, UK). Total RNA (1 µg/20 µL) was reverse transcribed using the Titanium One-Step real-time quantitative reverse transcription PCR (qRT-PCR) kit (Takara Bio, Inc., Kusatsu, Japan) according to the manufacturer's instructions. All selected genes were analyzed with the SYBR green detection method using the Stratagene Mx3000P real-time qPCR system (Stratagene, San Diego, CA, USA), and each sam-

Table 1 Primers used for qRT-PCR

Gene name	Forward primer (5'- to -3')	Reverse primer (5'- to -3')
DMP1	ggctacgacagaggccagta	tcctcatcgccaaggtatc
TNAP	tggtcacagcagttgtagc	tgacgttccgatcctgagtg
ANK	aactggcgaacacaagcaac	gcaaaggcaaagtccactcc
NPP1	ctgaccacagaagatgtagatgac	gaagggtgaagacgccaga
GAPDH	ttggcaaagtggagattgttg	ttcagctctgggatgacctt

Table 2 Number of mineralized nodules

Group	12 days	16 days	20 days	24 days
Blank control	22.67 ± 6.53	62.33 ± 6.08	99.00 ± 12.00	159.67 ± 20.02
siRNA control	21.00 ± 8.00*	61.00 ± 11.00*	96.00 ± 11.00*	155.33 ± 22.69*
siRNA	1.33 ± 0.58#	17.00 ± 5.00#	35.00 ± 7.00#	60.67 ± 9.08#

Data are presented as the mean ± SD. * $P > 0.05$ compared to the blank control. # $P < 0.01$ compared to the siRNA control.

ple was assayed in triplicate. Glyceraldehyde-3-phosphate dehydrogenase (GAPDH) served as a house-keeping/reference gene for target gene normalization, and gene expression levels were compared using relative quantification with corrected amplification efficiency for all primers. The primers are shown in **Table 1**. Data were analyzed using the $\Delta\Delta C_t$ method.

TNAP Activity Assay

We determined the protein content and specific activity of TNAP as described previously¹⁸. TNAP activity was measured after washing the MC3T3-E1 osteoblast cultures twice with phosphate-buffered saline before harvesting in 10 mM Tris (pH 7.4)/0.2% IGEPAL (Sigma-Aldrich, St. Louis, MO, USA). MC3T3-E1 cell lysates were obtained by sonication, and TNAP activity was measured using SIGMAFAST p-nitrophenyl phosphate tablets (Sigma-Aldrich) according to the manufacturer's instructions. TNAP from bovine intestinal mucosa (Sigma-Aldrich) was used as a standard, and TNAP activity was normalized to the protein content.

Alizarin Red Staining for Matrix Mineralization

MC3T3-E1 cells were fixed with 4% paraformaldehyde for 30 min at room temperature before staining with 2% alizarin red (Sigma-Aldrich) at pH 4.2. After the images were captured, the cells were destained with 10% cetylpyridinium chloride and the optical density was determined at 570 nm¹⁹. The conditions of nodule formation were routinely checked via phase-contrast microscopy (Nikon, Tokyo, Japan) at 100× magnification. Ten fields of view were retrieved. The experiments were performed in triplicate.

Matrix Vesicle Isolation

MC3T3-E1 cells were cultured for 10 days, and the medium was changed daily until day 7, after which 10 mL of medium was left in each plate until day 10. The medium was collected and initially centrifuged at 20,000 × *g* for 20 min at 4°C to precipitate cellular debris. Subsequently, the supernatant was retrieved and centrifuged at 100,000 × *g* for 1 h to isolate the matrix vesicle fraction, which was later resuspended in 0.4 mL lysis buffer (LB; 1% Triton X-100 in 0.2 M Tris base with 1.6 mM MgCl₂, pH 8.1)^{18,20}.

Analysis of PPI, Calcium, Inorganic Phosphate, Zinc, and Magnesium Levels

PPI levels were determined radiometrically and normalized to the DNA content of the cell, as described previously²¹. To determine intracellular PPI levels, the cells were rinsed and heated at 65°C for 45 min, before rinsing again and lysing in LB. Extracellular PPI levels were determined from conditioned media treated in the same manner¹⁸. Levels of calcium (Ca²⁺), inorganic phosphate (Pi), zinc (Zn²⁺), and magnesium (Mg²⁺) were assessed using standard laboratory techniques (BioVision, Milpitas, CA, USA; Roche/Hitachi 747, Tokyo, Japan).

DMP1 Enzyme-Linked Immunosorbent Assay

To measure DMP1 protein levels, we developed an enzyme-linked immunosorbent assay method that uses plates coated with a monoclonal antibody against native DMP1 (Chemicon, Temecula, CA, USA) diluted 1:2,500 in 100 µL/well of 0.1 mol/L sodium bicarbonate at pH 9.0 and 4°C overnight. The wells were blocked with 10 mmol/L Tris, and 150 mmol/L NaCl and 0.05% Tween-

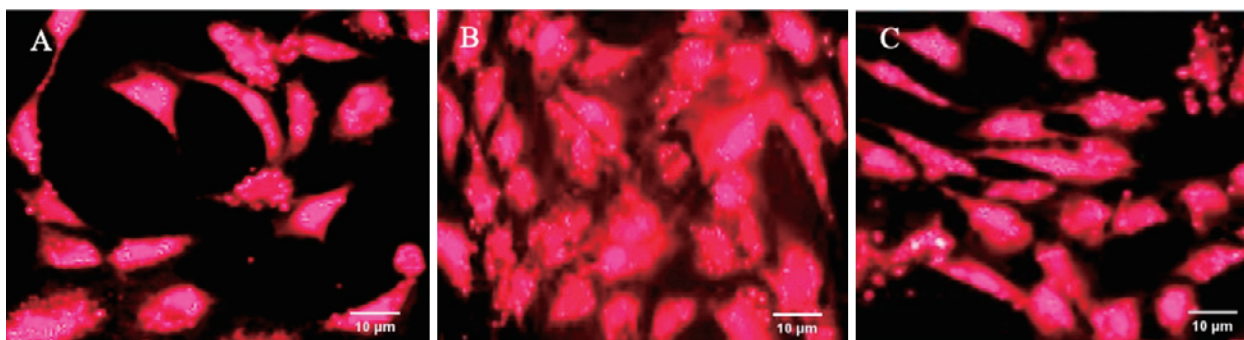


Fig. 1 Efficiency and optimal transfection concentrations of siRNA at (A) 20 nM, (B) 40 nM, and (C) 80 nM for MC3T3-E1 cells viewed under fluorescence microscopy.

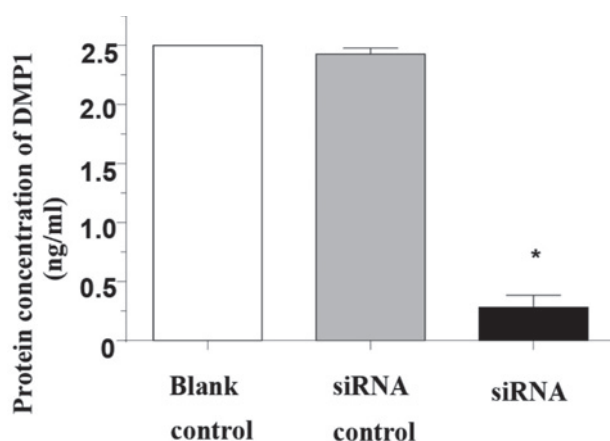


Fig. 2 DMP1 protein concentration in each group at 24 h after transfection (ng/mL). * $P < 0.01$.

20 (pH 8.0) were added and incubated for 1 h at 37°C. Recombinant murine DMP1 was used as the standard. The washed wells were incubated sequentially for 1 h at 37°C with Rabbit anti-DMP1 (1:1,000, Chemicon), followed by incubation with biotinylated goat anti-Rabbit IgG (1:1,000), and then streptavidin conjugated with alkaline phosphatase (1:500 dilution). The color was developed using *p*-nitrophenylphosphate and read at 405 nm.

Laboratory Assessment

Serum levels of Ca^{2+} , Pi , Zn^{2+} , and Mg^{2+} were assessed by standard laboratory techniques (BioVision; Roche/Hitachi 747).

Statistical Analysis

Statistical analysis was performed using SPSS software, version 20.0 (SPSS Inc., Chicago, IL, USA). All quantitative data are presented as mean \pm SD. The methods and assays were repeated at least three times to ensure the accuracy of the results. The statistical significance of differences among groups was determined by analysis of variance (ANOVA) and Scheffe's multiple-comparison techniques. Comparisons between time-based measure-

ments within each group were performed using repeated measures ANOVA. P -values < 0.05 were considered statistically significant.

Results

Efficiency and Optimal Transfection Concentration of siRNA for MC3T3-E1 Cells under Fluorescence Microscopy after Successful Transfection with siRNA

To determine the optimal transfection concentration, we tested red fluorescent dye at three concentrations (20, 40, and 80 nM), according to the manufacturer's instructions. Red fluorescence was emitted when the dye was successfully transfected into the cells. The transfection efficiencies were 70%, 90%, and 84%, respectively (Fig. 1 A~C). The transfection efficiency was highest at a dye concentration of 40 nM.

DMP1 Gene and Protein Expression after Transfection with siRNA Targeting DMP1

We measured the DMP1 protein concentration (ng/mL) in the cultured cells at 24 h after successful transfection. The results were as follows: blank control group, 2.497 ± 0.026 ; negative siRNA control group, 2.491 ± 0.025 ; and siRNA interference group, 0.257 ± 0.003 (Fig. 2).

Gene Expression of DMP1, TNAP, ANK, and ENPP1 in Cells after Transfection into Osteoblast MC3T3-E1 Cells with siRNA Targeting the DMP1 Gene

qRT-PCR was used to analyze gene expression levels of *DMP1*, *TNAP*, *ANK*, and *ENPP1*, and the data were analyzed using the $\Delta\Delta\text{Ct}$ method. We also applied repeated measurements and ANOVA to analyze the data. Statistical significance ($P < 0.01$) is indicated by an asterisk in the figures. After *DMP1* gene silencing, *DMP1* gene expression decreased, along with expression levels of *TNAP*, *ENPP1*, and *ANK* (Fig. 3A~D).

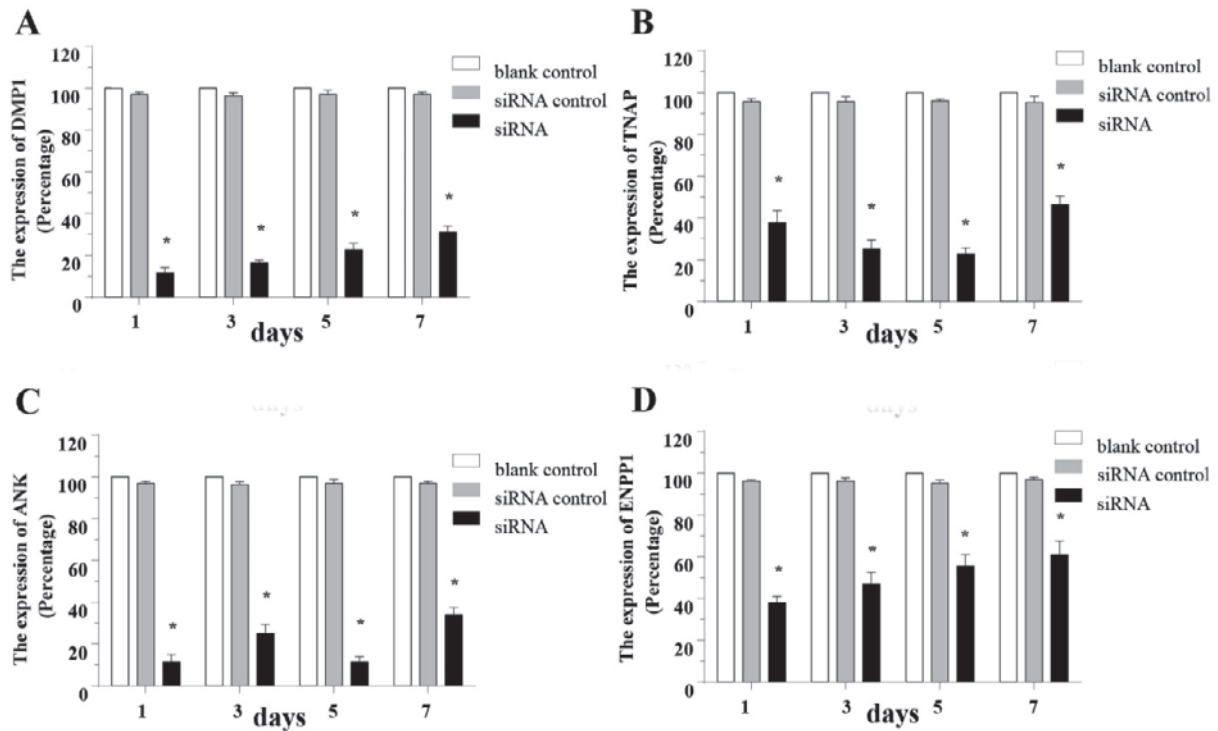


Fig. 3 mRNA expression (percentage of siRNA control) of (A) *DMP1*, (B) *TNAP*, (C) *ANK*, and (D) *ENPP1* in each group on days 1, 3, 5, and 7 of culture with mineralization medium. Data are presented as the mean \pm SD (n = 3). Comparison of mRNA expression levels between the siRNA control and blank control groups, $P > 0.05$; comparison of the mRNA expression levels between the siRNA and blank control groups, $P < 0.01$; comparison of the mRNA expression levels between the siRNA and siRNA control groups, $P < 0.01$.

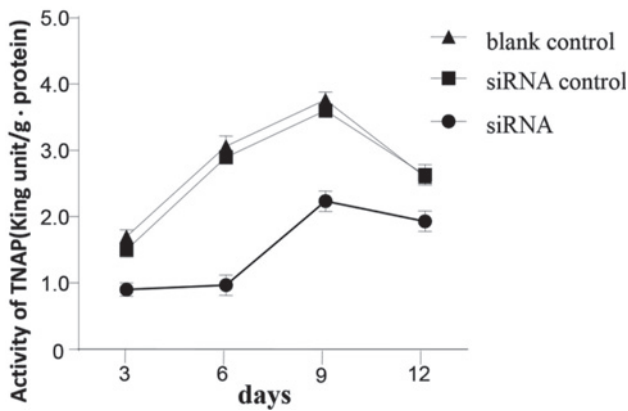


Fig. 4 TNAP activity in supernatant on days 3, 6, 9, and 12 of cell culture with mineralization medium. Data are presented as the mean \pm SD (n = 3). Comparison of TNAP activity between the siRNA control and blank control groups, $P > 0.05$; comparison of TNAP activity between the siRNA and blank control groups, $P < 0.01$; comparison of TNAP activity between the siRNA and siRNA control groups, $P < 0.01$.

Effect of Transfection with siRNA Targeting the *DMP1* Gene on TNAP Activity

MC3T3-E1 cells were cultured in a mineralization medium. Throughout the induction period, TNAP activity

first increased and then decreased, reaching a peak on day 9. TNAP activity was lower in the siRNA group than in the blank control and siRNA control groups. A P value of < 0.01 was considered statistically significant. After transfection with siRNA, TNAP activity underwent a refractory period from day 3 through day 6 (Fig. 4).

Mineralization Analysis

On day 7 of culture with mineralization medium, an inverted microscope was used to observe cells at the bottom of the bottle. On days 12, 16, 20, and 24 of culture, cells were stained with alizarin red and observed with an inverted microscope, before capturing images with a camera (data not shown). On day 12 of culture, scattered orange mineralized nodules were observed in the blank control and siRNA control groups. However, the siRNA group showed a few mineralized nodules. As the mineralization induction time progressed, the number of mineralized nodules increased (Fig. 5, Table 2).

Analysis of Intravesicular, Extravesicular, and Extracellular Matrix Levels of PPi , Pi , Ca^{2+} , Mg^{2+} , and Zn^{2+}

Next, the effect of transfection with siRNA on the ability of *DMP1* to influence intravesicular, extravesicular, and ECM levels of PPi , Pi , Ca^{2+} , Zn^{2+} , and Mg^{2+} was investigated in MC3T3-E1 cells. We transfected MC3T3-E1

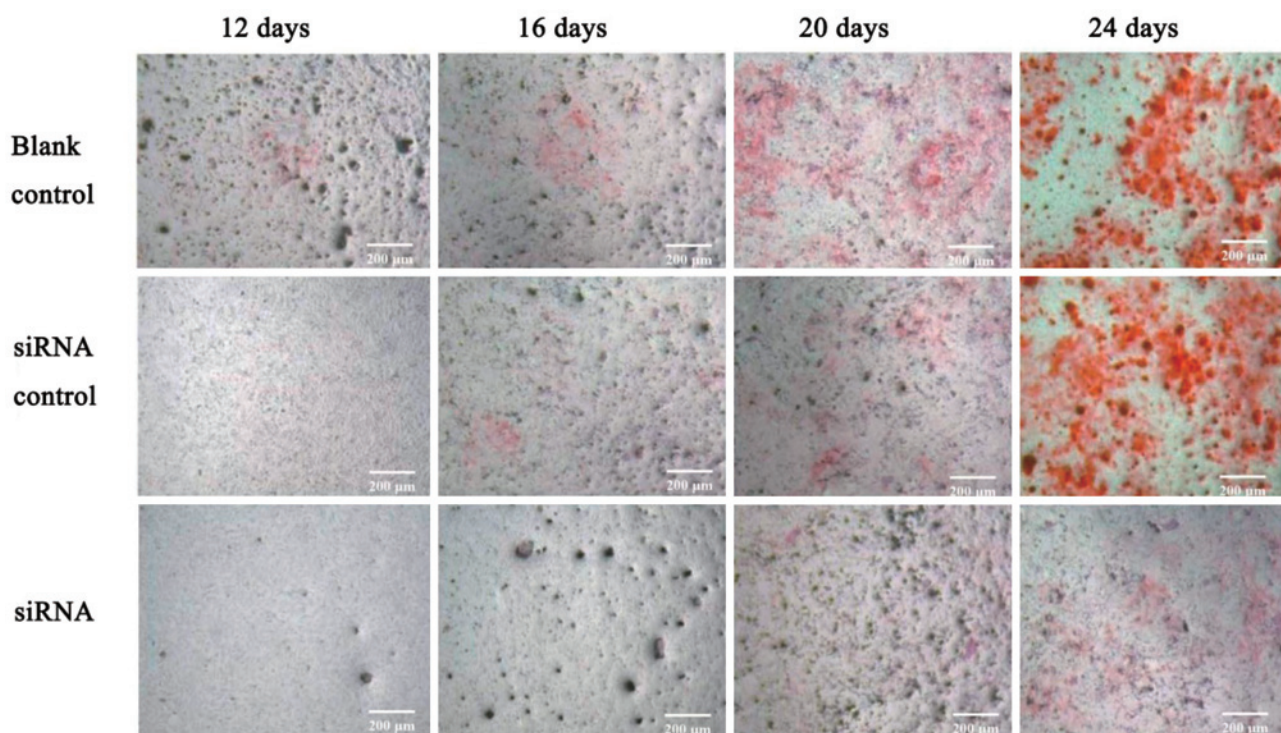


Fig. 5 Mineralized nodules (40 \times) stained with alizarin red were observed under an inverted microscope.

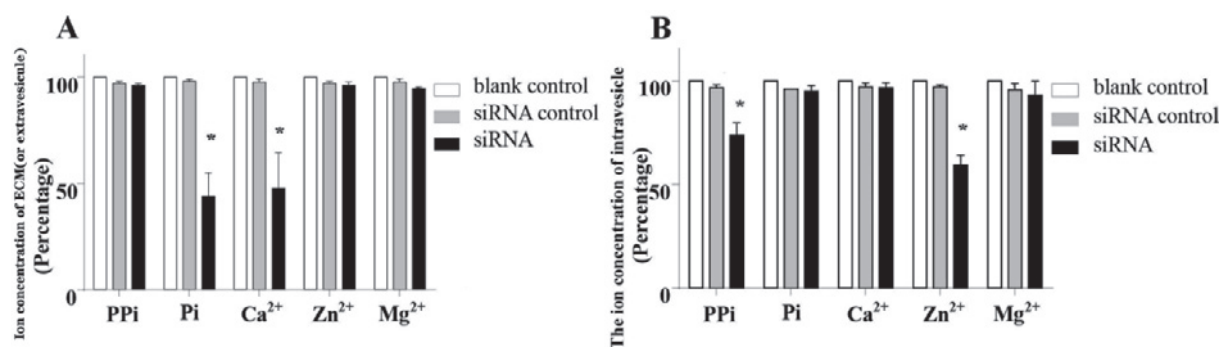


Fig. 6 ECM (or extravesicular) and intravesicular matrix levels of PPI, Pi, Ca²⁺, Mg²⁺, and Zn²⁺ in MC3T3-E1 cells. (A) ECM (or extravesicular) ion concentration (percentage); (B) intravesicular ion concentration (percentage).

cells with siRNA targeting DMP1 or blank siRNA, as described in the Materials and Methods, after 48 h of culture. Extravesicular and ECM levels of PPI, Mg²⁺, and Zn²⁺ remained constant but Pi and Ca²⁺ levels decreased. Moreover, intravesicular levels of Zn²⁺ and PPI decreased, while Pi, Mg²⁺, and Ca²⁺ levels remained constant, as compared with the siRNA control group (Fig. 6A, B; **P* < 0.01 vs siRNA controls).

Discussion

DMP1 Promotes Expression of TNAP, ENPP1, and ANK through Transcriptional Pathways

The functional differentiation of odontoblasts requires unique sets of genes to be turned on and off in a

differentiation-specific manner⁷. We observed that after gene silencing of DMP1, expression of DMP1, TNAP, ENPP1, and ANK was reduced. Narayanan et al.²² reported that DMP1 is primarily located in the nuclei, where it acts as a transcription factor for activation of osteoblast-specific genes and is responsible for transcription of matrix genes involved in the formation of mineralized tissue. On the basis of findings from overexpression studies, Narayanan et al.⁷ speculated that DMP1 may directly activate transcriptional pathways, leading to expression of TNAP in osteoblasts. In the nucleus, DMP1 is responsible for transcription of matrix genes involved in mineralized tissue formation. However, the mechanism by which DMP1 is taken up by osteoblasts is un-

known. TNAP, ENPP1, and ANK are well-characterized markers of osteoblast lineage mineralization, differentiation, and maturation. Previous findings, including those of our group, suggest that DMP1 may directly activate transcriptional pathways, leading to expression of TNAP, ANK, and ENPP1 in MC3T3-E1 cells, and that DMP1 may combine with an enhancer or transcription factor of TNAP, ANK, and ENPP1 in the nucleus of MC3T3-E1, thereby affecting expression of the three genes, which should be verified in further research.

DMP1 May Affect TNAP Activity via Regulation of Zn²⁺ Transporters

TNAP is a compact, dimeric enzyme with four metal-binding sites in or near the catalytic region of each subunit. The catalytic site of each subunit contains two Zn²⁺ ions and one Mg²⁺ ion, while a stabilizing Ca²⁺ ion is located 10 Å from the active site²³. Fujimoto et al.²⁴ suggested that cooperative Zn²⁺ handling by zinc transporter 1, metallothionein, and zinc transporter 4 in cytoplasm is required for full activation of TNAP, demonstrating that the activation process of TNAP is elaborately controlled. Importantly, Zn²⁺ is remarkably abundant in matrix vesicles²⁵.

In our study, TNAP activity in MC3T3-E1 cells treated with βGP and ascorbic acid increased, reached a peak on day 9, and decreased thereafter. This finding demonstrates that βGP (a source of phosphate for mineralization) can promote TNAP activity. TNAP activity was lower in the DMP1 siRNA interference group than in the blank control and siRNA control groups. Notably, after transfection with siRNA, TNAP activity underwent a refractory period from day 3 through day 6 (Fig. 4), and the concentration of intravesicular Zn²⁺ decreased after transfection with siRNA (Fig. 6B). This finding suggests that DMP1 affects TNAP activity by regulating Zn²⁺ transporters, especially in the early stage of interference. Nishito et al.²⁶ observed that zinc transporter 1 expression on the cell surface was elaborately controlled by intracellular zinc levels. DMP1 may regulate these transporters involved in Zn²⁺ uptake, likely in the matrix vesicles before mineralization formation. Therefore, DMP1 affects the activity of TNAP in two ways—by rapid ZnT regulation, during the initial stage, and by hysteresis transcriptional regulation, during the later stage.

After Treatment of MC3T3-E1 Cells with siRNA, Extravesicular Low Pi Switches Off the Pi/PPi-TNAP-Positive Feedback Loop before a High Pi/PPi Ratio Is Reached

The concentration of extracellular PPI is primarily

regulated by the action of TNAP, ENPP1, and ANK. TNAP decreases PPI levels by cleaving PPI to generate Pi, resulting in a high Pi/PPI ratio; this promotes mineralization and TNAP activity, which is a positive feedback process (Fig. 7). ENPP1 and ANK assist with inhibiting calcification, TNAP activity, and the emergence of Pi/PPI-TANP-positive feedback by increasing the concentration of extracellular PPI²⁷. Mice lacking ANK exhibit an arthritis-like phenotype characterized by ectopic calcifications in cartilage and joint tissues¹⁴. Moreover, mice lacking ENPP1 exhibit mineralization in the arteries and kidneys and ectopic formation of cartilage in the joints and spine²⁸. A previous study showed that oral SBI-425, a selective TNAP inhibitor, inhibited development of arterial media calcification in mice, without affecting bone mineralization²⁹. Thus, lack of ENPP1 and ANK promotes mineralization, TNAP activity, and the emergence of Pi/PPI-TANP-positive feedback. In other words, a high Pi/PPI ratio promotes positive feedback, whereas a low Pi/PPI ratio inhibits it. Reduced expression of ENPP1 and ANK decreases the production of PPI. Additionally, hydrolysis of PPI is reduced because of the decreased function of TNAP. Therefore, in the present study, PPI concentration was constant in the ECM (Fig. 6A). DMP1 affects the activity of TNAP in two ways—by rapid ZnT regulation, in the initial stage, and hysteresis transcriptional regulation, in the later stage. However, DMP1 may only affect expression of ENPP1 and ANK by hysteresis transcriptional regulation. Thus, the change in Pi/PPI caused by TNAP always occurs earlier than that of Pi/PPI caused by ENPP1 and ANK. Low extravesicular Pi switches off the Pi/PPI-TNAP-positive feedback after treatment of MC3T3-E1 cells with siRNA, before reaching a high Pi/PPI ratio, because of the lack of ENPP1 and ANK. This explains why, after transfection with siRNA, the activity of TNAP underwent a refractory period from day 3 through day 6 (Fig. 4).

In summary, DMP1 may regulate mineralization of MC3T3-E1 cells via the TNAP-ANK-ENPP1 axis, which results in unique sets of genes being turned on and off, low and high levels of ions, Pi/PPI-TNAP-positive feedback being switched on and off, self-phosphorylation, and conformational changes (Fig. 7). These results highlight a promising target for regulating HA crystal growth during mineralization and lay the foundation for further studies of potential therapeutic targeting of these proteins in the treatment of disorders of mineralization, such as AS and OA. An understanding of the regulatory mechanisms that control the physiological process of

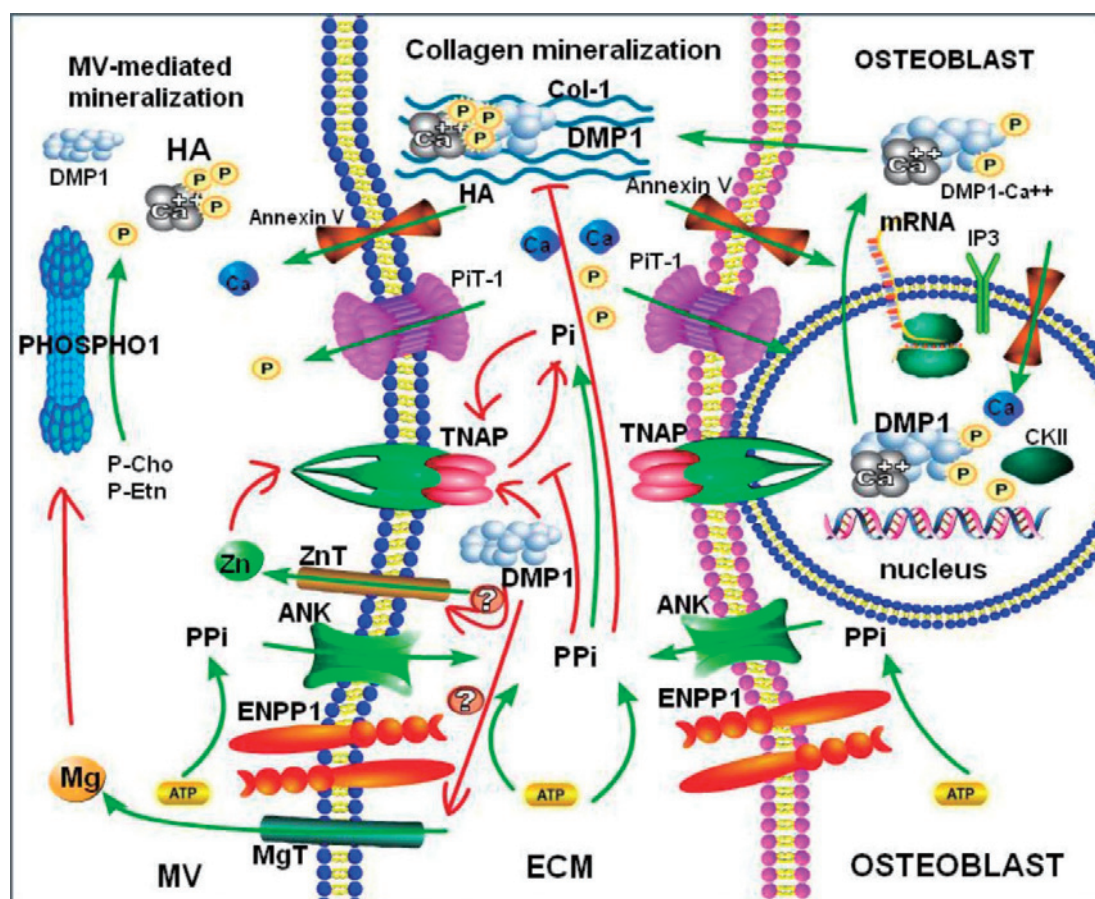


Fig. 7 DMP1 regulated mineralization of MC3T3-E1 cells via the TNAP-ANK-ENPP1 axis. MV = matrix vesicle.

biomineralization is necessary to better understand skeletal disorders and guide the development of therapeutics for treating pathological calcification.

Author contributions: JML and JHZ conceived the research and designed the experimental work with support from LZ; JML and JHZ performed the experiments with support from ZL (optimization of methods), HMW (experiments), and BBW and WL (results analysis); JML and LZ wrote and revised the manuscript for the final version to be published. All authors agree to be accountable for all aspects of the work.

Acknowledgements: This work was supported by the National Natural Science Foundation of China (No. 81371920), the Foundation of Liaoning Educational Committee (No. LJKZ 0821), the Natural Science Foundation of Liaoning Province (No. 2013022060), and the Principal Fund of Jinzhou Medical University.

Conflict of Interest: All authors declare that they have no competing interests.

References

1. Mebarek S, Hamade E, Thouverey C, et al. Ankylosing spondylitis, late osteoarthritis, vascular calcification, chondrocalcinosis and pseudo gout: toward a possible drug therapy. *Current medicinal chemistry* [Internet]. 2011;18(14):2196–203. Available from: <http://www.ncbi.nlm.nih.gov/pubmed/21517761>
2. Zhang W, Doherty M, Bardin T, et al. European League Against Rheumatism recommendations for calcium pyrophosphate deposition. Part I: terminology and diagnosis. *Annals of the rheumatic diseases* [Internet]. 2011 Apr;70(4):563–70. Available from: <http://www.ncbi.nlm.nih.gov/pubmed/21216817>
3. Richette P, Bardin T, Doherty M. An update on the epidemiology of calcium pyrophosphate dihydrate crystal deposition disease. *Rheumatology* [Internet]. 2009 Jul;48(7):711–5. Available from: <http://www.ncbi.nlm.nih.gov/pubmed/19398486>
4. Linde A, Goldberg M. Dentinogenesis. *Crit Rev Oral Biol Med* [Internet]. 1993;4(5):679–728. Available from: <http://www.ncbi.nlm.nih.gov/pubmed/8292714>
5. Ling Y, Rios HF, Myers ER, Lu Y, Feng JQ, Boskey AL. DMP1 depletion decreases bone mineralization in vivo: an FTIR imaging analysis. *J Bone Miner Res* [Internet]. 2005 Dec;20(12):2169–77. Available from: <https://www.ncbi.nlm.nih.gov/pubmed/16294270>
6. Liu T, Wang J, Xie X, et al. DMP1 ablation in the rabbit results in mineralization defects and abnormalities in

- Haversian canal/osteon microarchitecture. *J Bone Miner Res* [Internet]. 2019 Jun;34(6):1115–28. Available from: <http://www.ncbi.nlm.nih.gov/pubmed/30827034>
7. Narayanan K, Srinivas R, Ramachandran A, Hao J, Quinn B, George A. Differentiation of embryonic mesenchymal cells to odontoblast-like cells by overexpression of dentin matrix protein 1. *Proc Natl Acad Sci U S A* [Internet]. 2001 Apr 10;98(8):4516–21. Available from: <https://www.ncbi.nlm.nih.gov/pubmed/11287660>
 8. Bhatia A, Albazzaz M, Espinoza Orias AA, et al. Overexpression of DMP1 accelerates mineralization and alters cortical bone biomechanical properties in vivo. *J Mech Behav Biomed Mater* [Internet]. 2012 Jan;5(1):1–8. Available from: <https://www.ncbi.nlm.nih.gov/pubmed/22100074>
 9. Merkel A, Chen Y, George A. Endocytic trafficking of DMP1 and GRP78 complex facilitates osteogenic differentiation of human periodontal ligament stem cells. *Front Physiol* [Internet]. 2019;10:1175. Available from: <https://www.ncbi.nlm.nih.gov/pubmed/31572220>
 10. Liu JM, Cui YZ, Zhang GL, et al. Association between dentin matrix protein 1 (rs10019009) polymorphism and ankylosing spondylitis in a Chinese Han population from Shandong province. *Chin med J (Engl)* [Internet]. 2016 Mar 20;129(6):657–64. Available from: <http://www.ncbi.nlm.nih.gov/pubmed/26960368>
 11. Hui M, Tenenbaum HC. New face of an old enzyme: alkaline phosphatase may contribute to human tissue aging by inducing tissue hardening and calcification. *Anat Rec* [Internet]. 1998 Jun;253(3):91–4. Available from: <https://www.ncbi.nlm.nih.gov/pubmed/9700394>
 12. Liu CH, Raj S, Chen CH, et al. HLA-B27-mediated activation of TNAP phosphatase promotes pathogenic syndesmophyte formation in ankylosing spondylitis. *J Clin Invest* [Internet]. 2019 Dec 2;129(12):5357–73. Available from: <https://www.ncbi.nlm.nih.gov/pubmed/31682238>
 13. Johnson K, Goding J, Van Etten D, et al. Linked deficiencies in extracellular PP(i) and osteopontin mediate pathologic calcification associated with defective PC-1 and ANK expression. *J Bone Miner Res* [Internet]. 2003 Jun;18(6):994–1004. Available from: <https://www.ncbi.nlm.nih.gov/pubmed/12817751>
 14. Gurley KA, Chen H, Guenther C, et al. Mineral formation in joints caused by complete or joint-specific loss of ANK function. *J Bone Miner Res* [Internet]. 2006 Aug;21(8):1238–47. Available from: <https://www.ncbi.nlm.nih.gov/pubmed/16869722>
 15. Szeri F, Lundkvist S, Donnelly S, et al. The membrane protein ANKH is crucial for bone mechanical performance by mediating cellular export of citrate and ATP. *PLoS Genet* [Internet]. 2020 Jul;16(7):e1008884. Available from: <http://www.ncbi.nlm.nih.gov/pubmed/332639996>
 16. Hasegawa T, Yamamoto T, Tsuchiya E, et al. Ultrastructural and biochemical aspects of matrix vesicle-mediated mineralization. *Jpn Dent Sci Rev* [Internet]. 2017 May;53(2):34–45. Available from: <https://www.ncbi.nlm.nih.gov/pubmed/28479934>
 17. Nagasaki A, Nagasaki K, Chu EY, et al. Ablation of pyrophosphate regulators promotes periodontal regeneration. *J Dent Res* [Internet]. 2021 Jun;100(6):639–47. Available from: <http://www.ncbi.nlm.nih.gov/pubmed/33356859>
 18. Johnson K, Moffa A, Chen Y, Pritzker K, Goding J, Terkeltaub R. Matrix vesicle plasma cell membrane glycoprotein-1 regulates mineralization by murine osteoblastic MC3T3 cells. *J Bone Miner Res* [Internet]. 1999 Jun;14(6):883–92. Available from: <https://www.ncbi.nlm.nih.gov/pubmed/10352096>
 19. Staines KA, Mackenzie NC, Clarkin CE, et al. MEPE is a novel regulator of growth plate cartilage mineralization. *Bone* [Internet]. 2012 Sep;51(3):418–30. Available from: <http://www.ncbi.nlm.nih.gov/pubmed/22766095>
 20. Konoshenko MY, Lekhnov EA, Vlassov AV, Laktionov PP. Isolation of extracellular vesicles: general methodologies and latest trends. *Biomed Res Int* [Internet]. 2018;2018:8545347. Available from: <https://www.ncbi.nlm.nih.gov/pubmed/29662902>
 21. Terkeltaub R, Lotz M, Johnson K, et al. Parathyroid hormone-related proteins is abundant in osteoarthritic cartilage, and the parathyroid hormone-related protein 1-173 isoform is selectively induced by transforming growth factor beta in articular chondrocytes and suppresses generation of extracellular inorganic pyrophosphate. *Arthritis Rheum* [Internet]. 1998 Dec;41(12):2152–64. Available from: <https://www.ncbi.nlm.nih.gov/pubmed/9870872>
 22. Narayanan K, Ramachandran A, Hao J, et al. Dual functional roles of dentin matrix protein 1. Implications in biomineralization and gene transcription by activation of intracellular Ca²⁺ store. *J Biol Chem* [Internet]. 2003 May 9;278(19):17500–8. Available from: <https://www.ncbi.nlm.nih.gov/pubmed/12615915>
 23. Llinas P, Stura EA, Menez A, et al. Structural studies of human placental alkaline phosphatase in complex with functional ligands. *J Mol Biol* [Internet]. 2005 Jul 15;350(3):441–51. Available from: <https://www.ncbi.nlm.nih.gov/pubmed/15946677>
 24. Fujimoto S, Isumura N, Tsuji T, et al. Cooperative functions of ZnT1, metallothionein and ZnT4 in the cytoplasm are required for full activation of TNAP in the early secretory pathway. *PLoS One* [Internet]. 2013;8(10):e77445. Available from: <https://www.ncbi.nlm.nih.gov/pubmed/24204829>
 25. Sauer GR, Adkisson HD, Genge BR, Wuthier RE. Regulatory effect of endogenous zinc and inhibitory action of toxic metal ions on calcium accumulation by matrix vesicles in vitro. *Bone Miner* [Internet]. 1989 Nov;7(3):233–44. Available from: <https://www.ncbi.nlm.nih.gov/pubmed/2611445>
 26. Nishito Y, Kambe T. Zinc transporter 1 (ZNT1) expression on the cell surface is elaborately controlled by cellular zinc levels. *J Biol Chem* [Internet]. 2019 Oct 25;294(43):15686–97. Available from: <https://www.ncbi.nlm.nih.gov/pubmed/31471319>
 27. Addison WN, Azari F, Sorensen ES, Kaartinen MT, McKee MD. Pyrophosphate inhibits mineralization of osteoblast cultures by binding to mineral, up-regulating osteopontin, and inhibiting alkaline phosphatase activity. *J Biol Chem* [Internet]. 2007 May 25;282(21):15872–83. Available from: <http://www.ncbi.nlm.nih.gov/pubmed/17383965>
 28. Mackenzie NC, Zhu D, Milne EM, et al. Altered bone development and an increase in FGF-23 expression in Enpp1(-/-) mice. *PLoS One* [Internet]. 2012;7(2):e32177. Available from: <https://www.ncbi.nlm.nih.gov/pubmed/22359666>
 29. Opdebeeck B, D'Haese PC, Verhulst A. Inhibition of tissue non-specific alkaline phosphatase, a novel therapy against arterial media calcification? *J Pathol* [Internet]. 2020 Mar;250(3):248–50. Available from: <https://www.ncbi.nlm.nih.gov/pubmed/31859361>

DMP1 Regulates MC3T3-E1 Cell Mineralization

(Received, October 9, 2022)

(Accepted, January 26, 2023)

Journal of Nippon Medical School has adopted the Creative Commons Attribution-NonCommercial-NoDerivatives 4.0 International License (<https://creativecommons.org/licenses/by-nc-nd/4.0/>) for this article. The Medical Association of Nippon Medical School remains the copyright holder of all articles. Anyone may download, reuse, copy, reprint, or distribute articles for non-profit purposes under this license, on condition that the authors of the articles are properly credited.
